Cell, Volume *131*

Supplemental Data

The ATPase SpoIIIE Transports DNA across Fused Septal Membranes during Sporulation in *Bacillus subtilis*

Briana M. Burton, Kathleen A. Marquis, Nora L. Sullivan, Tom A. Rapoport, and David Z. Rudner

Supplemental Experimental Procedures

Fluorescence microscopy

Fluorescence microscopy was performed as previously described (Rudner and Losick, 2002; Doan et al., 2005). Exposure times were typically 500 ms for SpoIIIE-GFP. Membranes were stained with either TMA-DPH or FM4-64 (Molecular Probes), at a final concentration of 0.01 mM, and imaged with exposure times of 200 ms and 300 ms respectively. Fluorescence images were analyzed, adjusted and cropped using Metamorph v 6.1 software (Molecular Devices). Forespores with YFP and CFP fluorescence were scored either as "on" or "off", after correction for background fluorescence.

Electron Microscopy

Wild type *B. subtilis* cells were induced to sporulate by resuspension. Two ml of culture was harvested and the cell pellets resuspended in 25 µl SMM buffer (0.5 M sucrose, 20 mM $MgSO_4$, 20 mM maleic acid, pH 6.5). Cells were high pressure frozen and freeze substituted essentially as described (Preble et al., 2001). Briefly, aliquots of cell pellets were transferred to the 0.2-mm deep well of aluminum planchettes (Technotrade International, Manchester, NH) and high-pressure-frozen in a BAL-TEC (Oerlikon, Balzers, Liechtenstein) HPM-010 High Pressure Freezer. The frozen samples were freeze-substituted in 0.25% glutaraldehyde/0.1% uranyl acetate in acetone at –80˚C for 3 days, then gradually warmed to –20˚C, infiltrated with Lowicryl HM20 embedding resin (EMS, Hatfield, PA), and finally polymerized in BEEM capsules under UV illumination at –45˚C. Sections with a nominal thickness of 60 nm were collected on formvar-coated copper or nickel (for immunolabeling) EM grids. The sections were immuno-stained with gold-conjugated anti-GFP antibodies. For immunolocalization of

the GFP-fusion proteins, sections on nickel grids were floated on blocking buffer consisting of 1% nonfat dry milk in PBS with 0.1% Tween 20 for 30 min, incubated for 2 h on anti-GFP primary antibody (J. Kahana and P. Silver, Harvard Medical School, Boston, MA) diluted 1:150 in blocking buffer, rinsed in PBST, then exposed to goat-anti-rabbit 20-nm gold secondary antibody (Ted Pella, Inc., Redding, CA) for 1 h and rinsed. All grids were stained with uranyl acetate and lead citrate, then viewed in a Tecnai G^2 Spirit BioTWIN operating at 80 kV. Images were recorded with an AMT 2k CCD camera.

Plasmid Construction

The plasmids used in this study are listed in Table S2.

pBB78 [*ycgO::spoIIIE (cat)*] was generated in a two-way ligation with an *Eco*RI-*Bam*HI PCR product containing the *spoIIIE* gene (oligonucleotide primers oBB162 and oBB163 and genomic DNA as template) and pKM77 cut with *Eco*RI and *Bam*HI. pKM77 [*ycgO::cat*] is an ectopic integration vector for double-crossover insertions into the nonessential *ycgO* locus (K.M. and D.Z.R., unpublished).

pBB152 [*PspoIIQ-cfp-yhdY (spec)*] was generated in a two-way ligation with a *Bam*HI-*Pst*I PCR product containing a portion of the *yhdY* gene (oligonucleotide primers oBB183 and oBB184 and genomic DNA as template) and pBB160 cut with *Bam*HI and *Pst*I. pBB160 [*PspoIIQ-cfp (spec)*] was generated in a two-way ligation with an *Eco*RI-*Bam*HI fragment containing *PspoIIQ-cfp* cut from pKM8 (Doan et al., 2005) and pUS19 cut with *Eco*RI and *Bam*HI.

pBB153 [*PspoIIQ-cfp-ytzH (spec)*] was generated in a two-way ligation with a *Bam*HI-*Pst*I PCR product containing a portion of the *ytzH* gene (oligonucleotide primers oBB181 and oBB182 and genomic DNA as template) and pBB160 cut with *Bam*HI and *Pst*I.

pBB155 [*PspoIIQ-yfp-ytzH (spec)*] was generated in a two-way ligation with a *Bam*HI-*Pst*I PCR product containing a portion of the *ytzH* gene (oligonucleotide primers oBB181 and oBB182 and genomic DNA as template) and pBB151 cut with *Bam*HI and *Pst*I. pBB151 [*PspoIIQ-yfp (spec)*] was generated in a two-way ligation with an *Eco*RI-*Bam*HI fragment containing *PspoIIQ-yfp* from pKM3 and pUS19 cut with *Eco*RI and *Bam*HI. pKM3 [*amyE::PspoIIQ-yfp(JF) (spec)*] was generated by two-way ligation with a PCR product amplified from pKL183 (Lemon et al., 2000) with oligonucleotides oDR78 and oDR107 and cut with *Hind*III and *Bam*HI cloned into pKM1 (Doan et al., 2005) cut with *Hind*III and *Bam*HI. pKM1 PspoIIQ promoter was amplified from pdr172a with oligos

odr234 and odr235. The PCR product was cut with HindIII and EcoRI and cloned into pLD30 (Garsin et al., 1998) between *Eco*RI and *Hind*III.

pBB156 [*PspoIIQ-yfp-yhdY (cat)*] was generated in a two-way ligation with a *Bam*HI-*Pst*I PCR product containing a portion of the *yhdY* gene (oligonucleotide primers oBB183 and oBB184 and genomic DNA as template) and pBB150 cut with *Bam*HI and *Pst*I. pBB150 [*PspoIIQ-yfp (cat)*] was generated in a two-way ligation with an *Eco*RI-*Bam*HI fragment containing *PspoIIQ-yfp* from pKM3 and pER19 (Ricca et al., 1992) cut with *Eco*RI and *Bam*HI.

pBB171 [*PspoIIQ-cfp-ydhY (kan)*] was generated in a two-way ligation with an *Xba*I-*Pst*I fragment containing *PspoIIQ-cfp-yhdY* from pBB152 into pUK19 cut with *Xba*I and *Pst*I.

pBB183 [*ycgO::spoIIIE(D584A) (cat)*] was generated by introducing the D584A mutation into the gene encoding *spoIIIE* by site-directed mutagenesis in pBB78 (oligonucleotides oBB148 and oBB149).

pBB198 [*PspoIIQ-yfp-ytzH (phleo)*] was generated in a two-way ligation with a *Xba*I-*Pst*I fragment containing *PspoIIQ-yfp-ytzH* cut from pBB155 and pTD2 cut with *Xba*I and *Pst*I.

pKM188 [*yycR::(tetO)120 (cat)*] was generated in a two-way ligation with a *Hind*III-*Xho*I PCR product amplified from pLAU44 (Lau et al., 2003), and pNS037 cut with *Hind*III-*XhoI*. pNS037 [*yycR::cat*] is an ectopic integration vector for double-crossover insertions into the nonessential *yycR* locus (N.L.S. and D.Z.R., unpublished).

pKM212 [*amyE::PspoIIE-tetR-gfp (spec)*] was generated in a two-way ligation with a *Bam*HI-*Hind*III PCR fragment containing *tetR-gfp* (oligonucleotide primers oDR78 and oDR188 and pBW3 as template (Dworkin and Losick, 2002),and pMF23 (Fujita and Losick, 2003) cut with *Bam*HI and *Hind*III.

pKM245 *ftsW-gfp (spec)* was generated by inserting a small fragment of *ftsW*, PCR amplified using oligonucleotides oDR575 and oDR577, into pKL147 (Lemon and Grossman, 1998) between *Eco*RI and *Xho*I.

pKM247 [*yycR::(tetO)12 (cat)*] was generated by two-way ligation of a *Hind*III-*Xho*I PCR product (amplified from pLAU44 using oligonucleotides oDR459 and oDR573) and pNS37 cut with *Hind*III-*Xho*I.

pKM248 [*yycR::(tetO)36 (cat)*] was generated by two-way ligation of a *Hind*III-*Xho*I PCR product (amplified from pLAU44 using oligonucleotides oDR459 and oDR574) and pNS37 cut with *Hind*III-*Xho*I.

pNS51 [*yycR::PspoIIQ-yfp (phleo)*] was generated by inserting *PspoIIQ-yfp* from pKM3 into pNS042 between *Eco*RI and *Bam*HI. pNS42 [*yycR::phleo*] is an ectopic integration vector for double-crossover insertions into the nonessential *yycR* locus (N.L.S. and D.Z.R., unpublished).

pNS56 [*pelB::PspoIIQ-cfp (kan)*] was generated in a two-way ligation with an *Eco*RI-*Bam*HI fragment cut from pKM8 (Doan et al., 2005) and pKM69 cut with *Eco*RI and *Bam*HI. pKM69 [*pelB::kan*] is an ectopic integration vector for double-crossover insertions into the nonessential *pelB* locus (K.M. and D.Z.R., unpublished).

pDT126 [*spoIIQ::cat*] a fragment containing the cat gene (for chlorampenicol resistance), digested by *Sal*I and *Bam*HI was inserted into pDT123a between *Sal*I and *Bam*HI (T. Doan and D.Z.R., unpublished).

Supplemental References

Broder, D.H., and Pogliano, K. (2006). Forespore engulfment mediated by a ratchet-like mechanism. Cell *126*, 917-928.

Doan, T., Marquis, K.A., and Rudner, D.Z. (2005). Subcellular localization of a sporulation membrane protein is achieved through a network of interactions along and across the septum. Mol Microbiol *55*, 1767-781.

Dworkin, J., and Losick, R. (2002). Does RNA polymerase help drive chromosome segregation in bacteria? Proc Natl Acad Sci U S A *99*, 14089-094.

Fujita, M., and Losick, R. (2003). The master regulator for entry into sporulation in Bacillus subtilis becomes a cell-specific transcription factor after asymmetric division. Genes Dev *17*, 1166-174.

Garsin, D.A., Paskowitz, D.M., Duncan, L., and Losick, R. (1998). Evidence for common sites of contact between the antisigma factor SpoIIAB and its partners SpoIIAA and the developmental transcription factor sigmaF in Bacillus subtilis. J Mol Biol *284*, 557-568.

Khvorova, A., Chary, V.K., Hilbert, D.W., and Piggot, P.J. (2000). The chromosomal location of the Bacillus subtilis sporulation gene spoIIR is important for its function. J Bacteriol *182*, 4425-29.

Lau, I.F., Filipe, S.R., Søballe, B., Økstad, O.A., Barre, F.X., and Sherratt, D.J. (2003). Spatial and temporal organization of replicating Escherichia coli chromosomes. Mol Microbiol *49*, 731-743.

Lemon, K.P., and Grossman, A.D. (1998). Localization of bacterial DNA polymerase: evidence for a factory model of replication. Science *282*, 1516-19.

Lemon, K.P., Kurtser, I., Wu, J., and Grossman, A.D. (2000). Control of initiation of sporulation by replication initiation genes in Bacillus subtilis. J Bacteriol *182*, 2989-991.

Nesmeyanova, M.A. (1982). On the possible participation of acid phospholipids in the translocation of secreted proteins through the bacterial cytoplasmic membrane. FEBS Lett *142*, 189-193.

Preble, A.M., Giddings, T.H., and Dutcher, S.K. (2001). Extragenic bypass suppressors of mutations in the essential gene BLD2 promote assembly of basal bodies with abnormal microtubules in Chlamydomonas reinhardtii. Genetics *157*, 163-181.

Ricca, E., Cutting, S., and Losick, R. (1992). Characterization of bofA, a gene involved in intercompartmental regulation of pro-sigma K processing during sporulation in Bacillus subtilis. J Bacteriol *174*, 3177-184.

Rudner, D.Z., and Losick, R. (2002). A sporulation membrane protein tethers the pro-sigmaK processing enzyme to its inhibitor and dictates its subcellular localization. Genes Dev *16*, 1007-018.

Zupancic, M.L., Tran, H., and Hofmeister, A.E. (2001). Chromosomal organization governs the timing of cell type-specific gene expression required for spore formation in Bacillus subtilis. Mol Microbiol *39*, 1471-481.

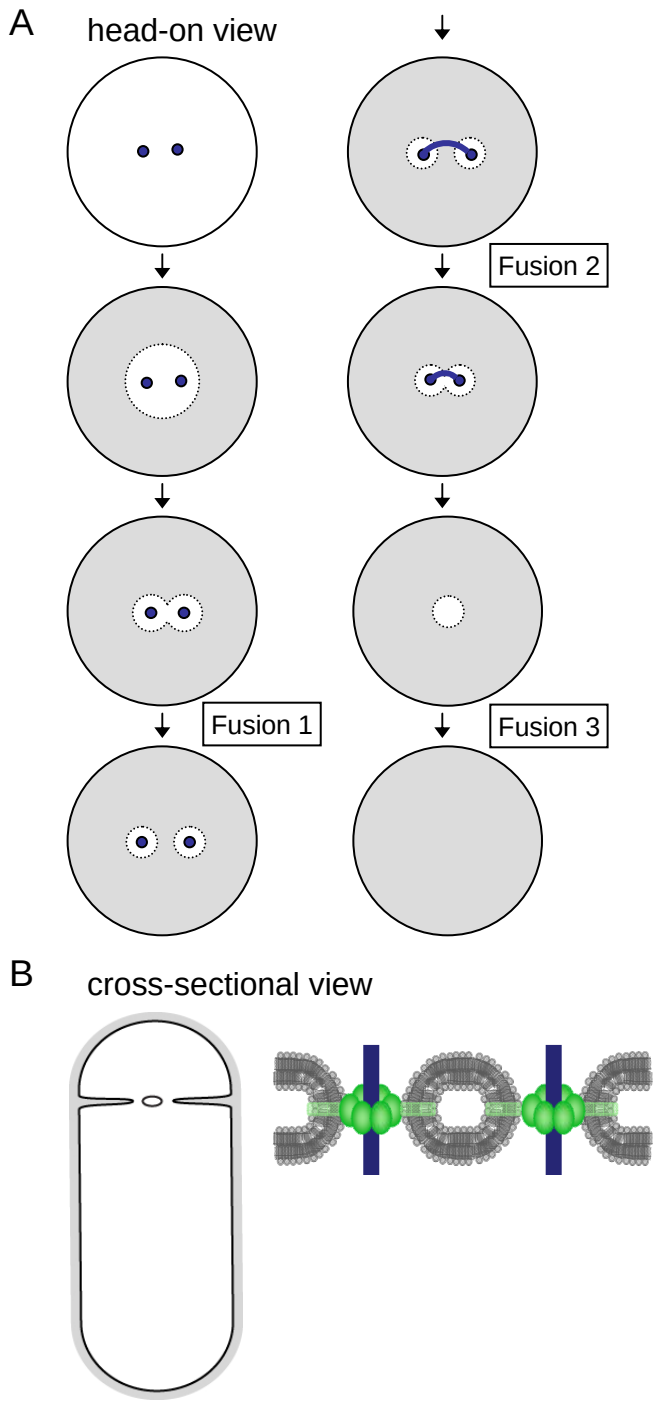

Figure S1 Model for SpoIIIE-dependent transport of the chromosome through two separate aqueous channels in the septum. This model requires three temporally distinct membrane fusion events. (A) Head-on view of the septum as observed from the mother-cell side. The constricting bilayers (light grey) close around the two chromosome arms (blue circles). The leading edge of the septal constriction is indicated by a dotted line. The first fusion event generates independent aqueous channels in the plane of the septal membrane. A second topologically distinct fusion event allows translocation of the final loop (blue line) of DNA. Finally the constricting membranes undergo a third fusion event to separate the mother cell and forespore. For simplicity SpoIIIE is not shown but would form separate hexameric rings around the DNA in the two channels. (B) Cross-sectional view shows the transmembrane segments of SpoIIIE anchoring the cytoplasmic ATPases domains in the two aqueous channels. The hexameric rings surround the two chromosome arms (blue lines).

Supplemental Figure 1 (Burton et al.)

Figure S2. SpoIIIE-GFP localizes throughout the cytoplasmic membranes early during sporulation. Cells containing SpoIIIE-GFP (strain BDR1626) were induced to sporulate by resuspension at 30˚C under conditions where sporulation proceeds slowly and analyzed at hour one by fluorescence microscopy. Membranes from the same field were visualized using the fluorescent dye FM4-64. The SpoIIIE-GFP image (middle panel) was scaled identically to the images in Figure 1C. To visualize the peripheral membrane localization of SpoIIIE-GFP the grey-scale levels were artificially increased (right panel).

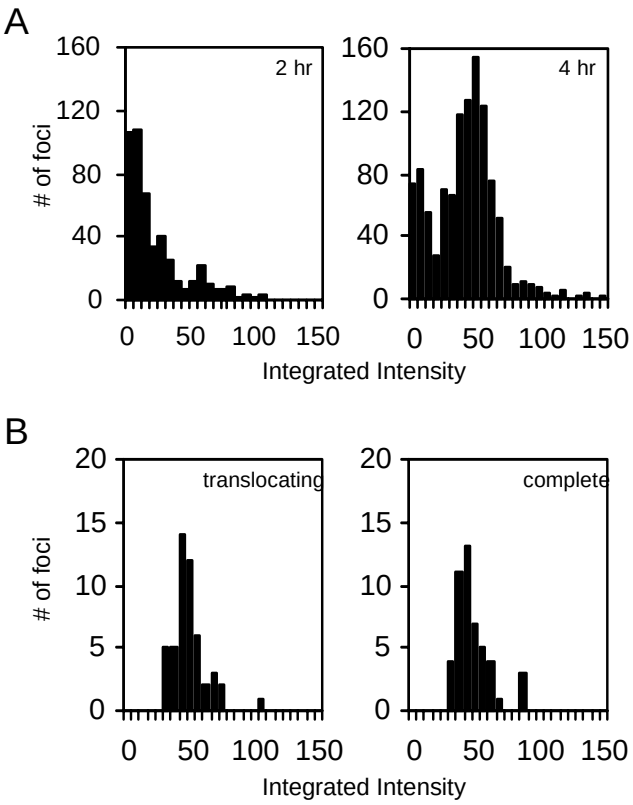

Figure 3S (A) Histograms plotting the integrated intensities of SpoIIIE-GFP foci from each sporulation time point. Three fluorescence micrographs from each time point (each micrograph contained several hundred sporangia) were corrected for background fluorescence and the integrated intensities of the GFP foci plotted. The peak at hour two, and the left peak at hour four consist of foci that were barely above the detection limit of the microscope, estimated to be 6-10 GFP molecules. Foci forming the main peak at hour four are 4- to 5-fold brighter than those in the peak at hour two, and therefore consist of at least 24-30 molecules. (B) Histograms plotting the fluorescence intensities of cells in the process of translocating DNA and cells that have completed DNA translocaton. Cells from hour four of sporulation were classified on the basis of DAPI staining into two categories: 1. Cells in the translocation process and 2. Cells that have completed translocation. The average intensities of the SpoIIIE foci for the two populations were very similar. Thus, the number of SpoIIIE molecules is at its maximum during DNA transport and remains constant until DNA transport is complete. (C) Histograms plotting the integrated fluorescence intensities of GFP foci from cells containing arrays of either 12, 36, or 120 *tetO* operator sites bound by TetR-GFP fusions. (D) Representative images of TetR-GFP bound to arrays of 12, 36 and 120 *tetO* operators and SpoIIIE-GFP foci at hour 1.5 of sporulation. Images are presented with the identical grey-scale range.

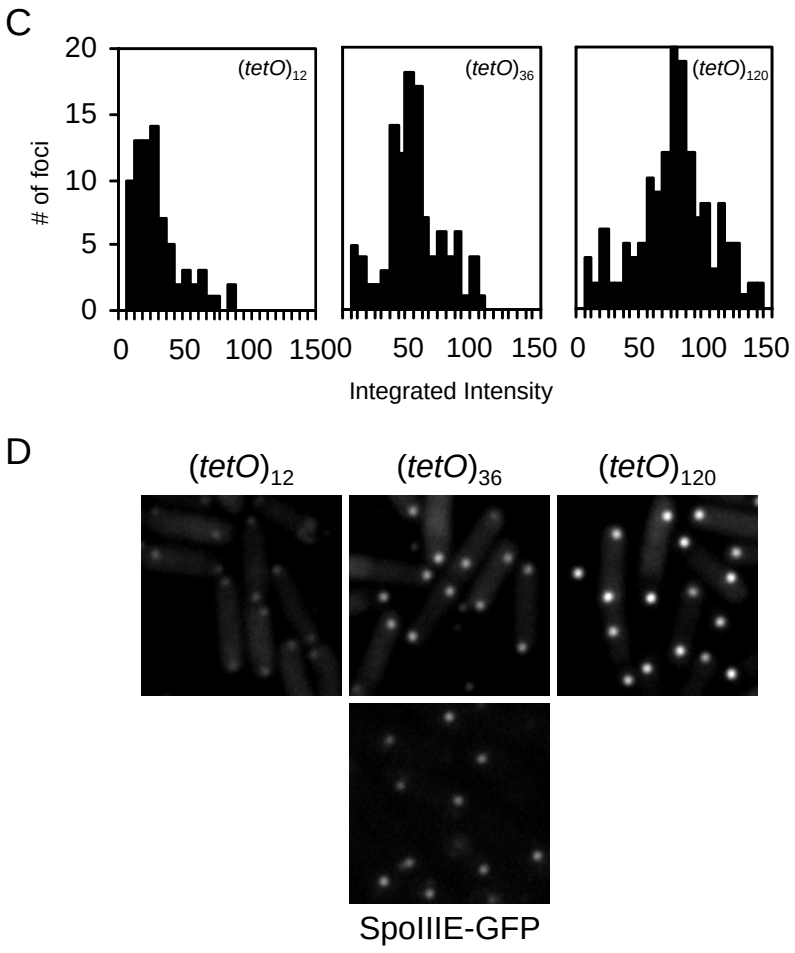

Supplemental Figure 3C&D (Burton et al.)

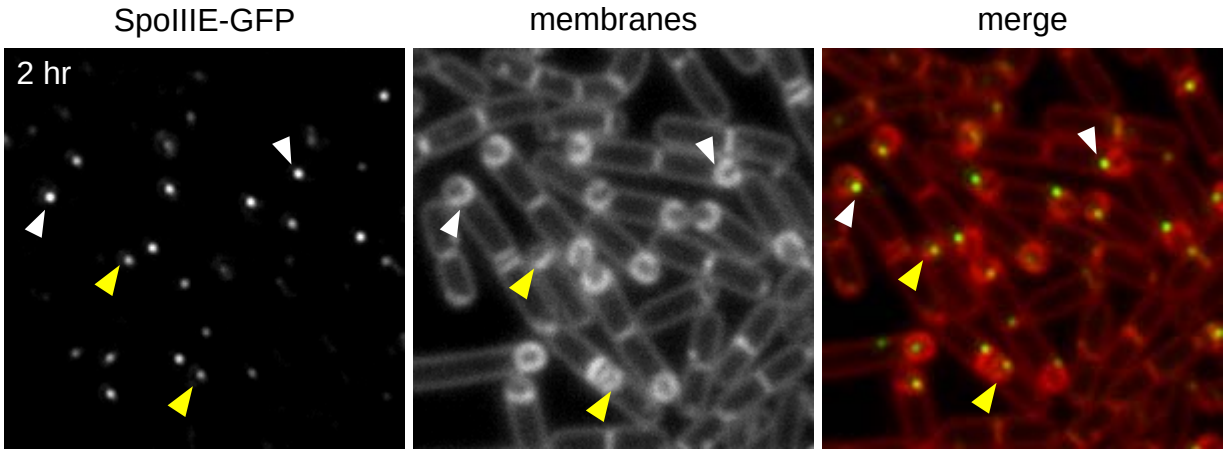

Figure S4. SpoIIIE-GFP foci increase in intensity under standard conditions of rapid sporulation at 37˚C. Cells containing SpoIIIE-GFP (strain BDR1626) were induced to sporulate by resuspension and analyzed at hour two by fluorescence microscopy. Faint SpoIIIE-GFP foci (yellow carets) that are seen at the time of septation and brighter foci that are seen during DNA translocation (white carets) are indicated. Membranes were visualized with FM4-64.

A

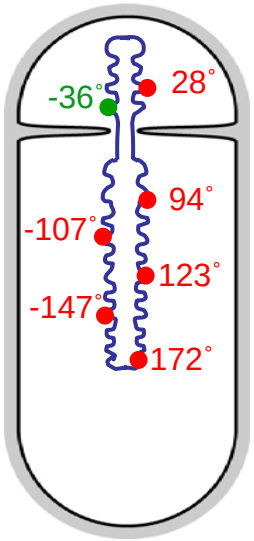

B

sporulation efficiency

Position	SpoIIIE+	IIIE(D584A)	Fold Δ
28˚	104%	101%	-
-36˚	100%	100%	-
94˚	90%	50%	1.8
-107˚	86%	52%	1.6
123˚	63%	22%	2.8
-147˚	48%	5%	9.6
172˚	20%	2%	10

Figure S5 Quantitative assessment of the slow pumping mutant SpoIIIE(D584A). Chromosome translocation was assessed by comparing sporulation efficiency in strains in which the *spoIIR* gene was placed at different sites in the chromosome. The *spoIIR* gene is located in the origin-proximal third of the chromosome (green dot, Figure S5A) and is activated by the forespore transcription factor sigmaF immediately after polar division. If *spoIIR* is moved to an origin-distal region, such that at the time of septation the *spoIIR* gene is not present in the forespore and therefore cannot be immediately activated by sigmaF, then sporulation is impaired. The further *spoIIR* is placed from the origin the longer it takes to be pumped into the forespore and the greater the sporulation defect (Figure S5B). Consistent with the idea that the SpoIIIE(D584A) mutant pumps the chromosome more slowly, the effect of moving *spoIIR* to origin-distal sites was greatly enhanced in this mutant background. The delay in *spoIIR* expression leads to the formation of a second polar septum. Accordingly, the disporic phenotype (yellow carets) was more pronounced in the slow pumping mutant (Figure S5C). Sporulation was induced by nutrient exhaustion in DSM. Sporulation efficiency was calculated as the number of spores compared to wild-type spores.

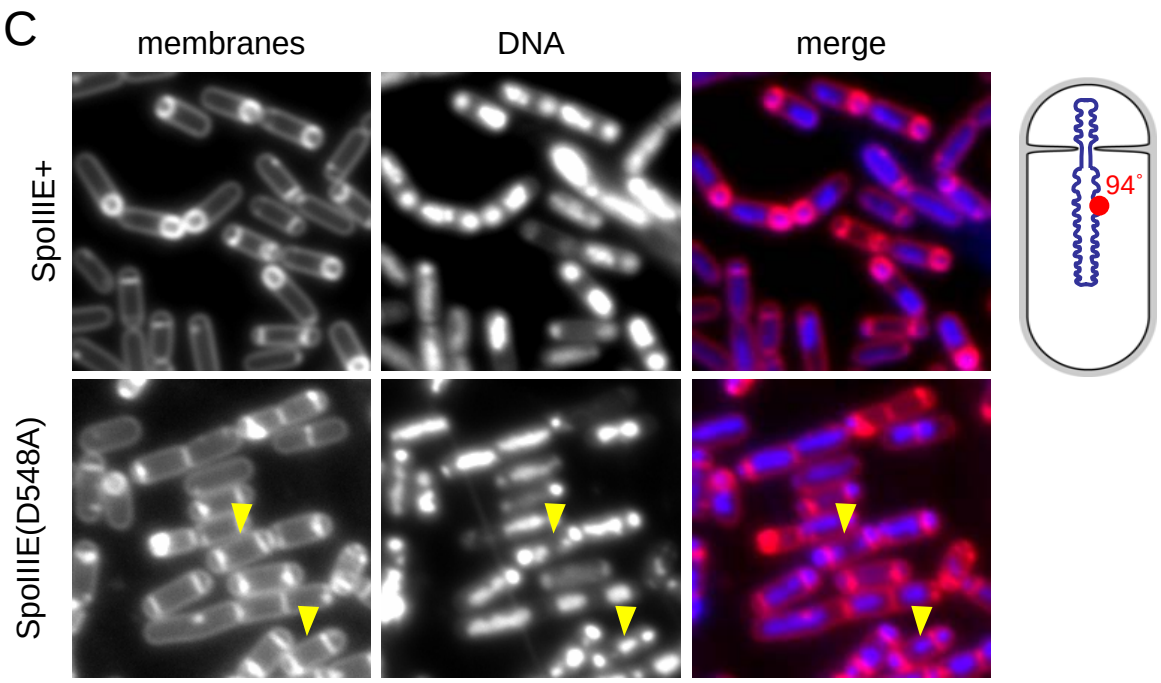

Supplemental Figure 5 (Burton et al.)

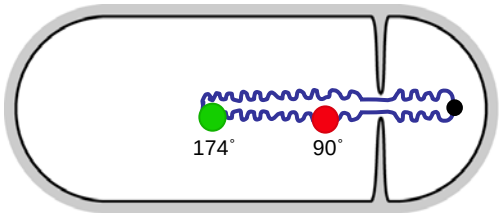

time (hr)	174˚ / 90˚
1.5	58%
2.0	86%

Figure S6. DNA transport is processive along the chromosome arm. Schematic of a sporulating cell used in this assay. For simplicity, only the chromosome transported by SpoIIIE is diagrammed. Red and green circles represent the location of the sigmaF-controlled reporter genes, *yfp* and *cfp*. The origin of the chromosome is marked with a black dot. The total number of forespores with CFP fluorescence (174˚ position) was compared to the number of forespores with YFP fluorescence (90˚ position) at 1.5 and 2 hours after the initiation of sporulation. The reporter closer to the origin was translocated into the forespore first.

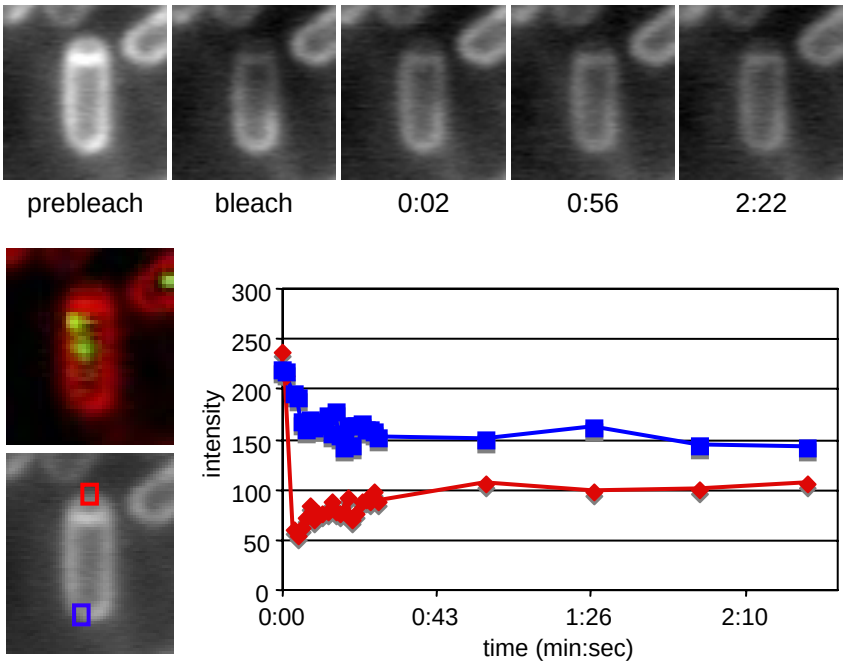

Figure S7. Wild-type sporulating cells that are actively translocating their DNA have completed membrane fusion. Analysis of lipid dynamics using FM4-64 and fluorescence recovery after photobleaching (FRAP). To ensure that SpoIIIE is actively translocating DNA, the 130˚ position of both chromosomes were visualized using an array of tet operators and TetR-GFP. Sporulating cells with two foci in the mother cell were selected for photobleaching, as these still have to move the marked chromosome region into the forespore. Image series above the graphs show the photobleaching time course. Images to the side of the graph show the foci of TetR-GFP bound to the *tetO* arrays at position 130˚ and the regions used for fluorescence quantitation. The graph shows forespore membrane (red diamonds) and mother-cell membrane (blue squares) fluorescence over the course of the experiment. Even after two minutes the fluorescent membrane dye in the mother cell membranes does not redistribute into the forespore membrane. This suggests that the membranes of the mother cell and forespore are no longer continuous. In this particular experiment immediately after photobleaching, there was a small amount of recovery of the forespore fluorescence. This is due to redistribution of fluorescence from the forespore side of the septum for which the photobleaching was incomplete.

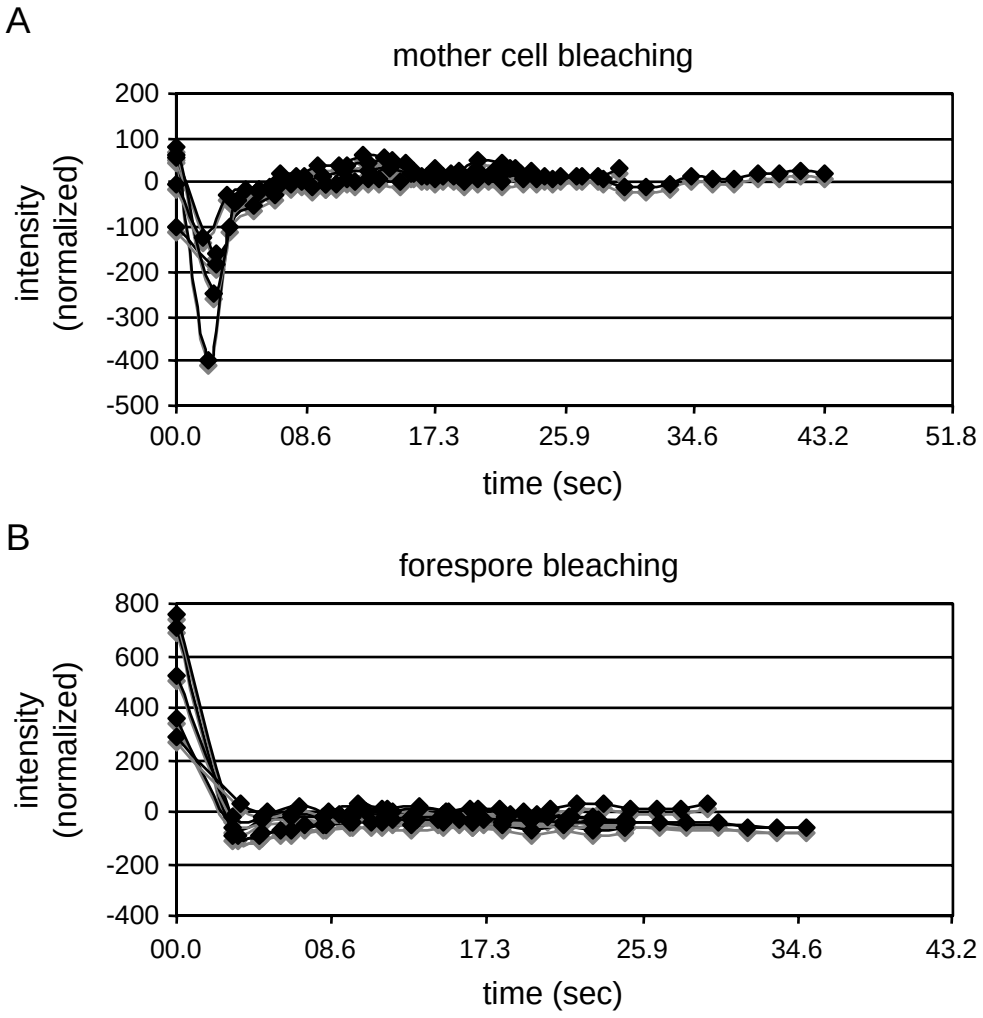

Figure S8. Photobleached forespore membranes reproducibly show no detectable recovery. Overlay of the photobleaching recovery curves of several cells from (A) mother-cell membrane bleaching, and (B) forespore membrane bleaching. The curves have been normalized around the plateaus. Note that even after 30 seconds, the bleached forespore membrane curves show no recovery.

A

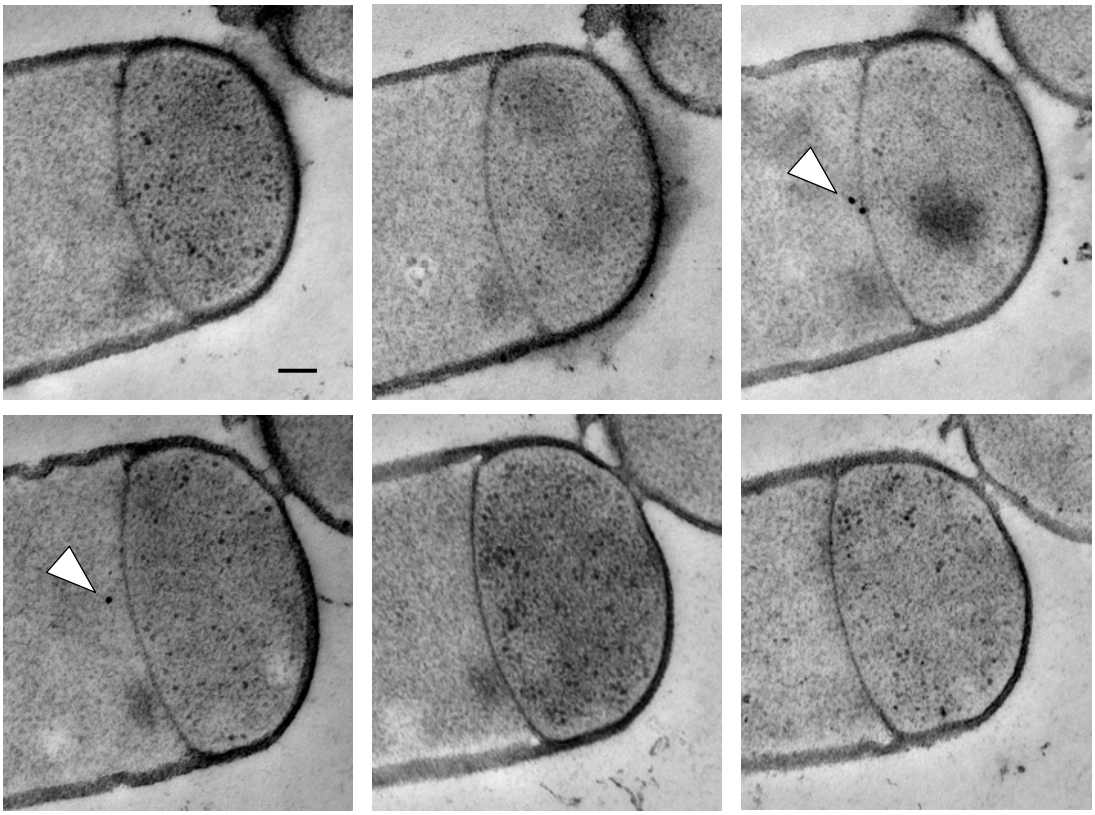

Figure S9. SpoIIIE-GFP is present on both sides of the septum. (A) Images from Figure 6A shown in a larger format. (B) Electron micrographs of sporulating cells expressing a functional *spoIIIE-gfp* fusion (strain BDR1626), immunostained with gold conjugated anti-GFP antibodies. SpoIIIE-GFP is detectable (carets) on both the mother cell and forespore sides of the septum. Scale bar is 100 nm.

B

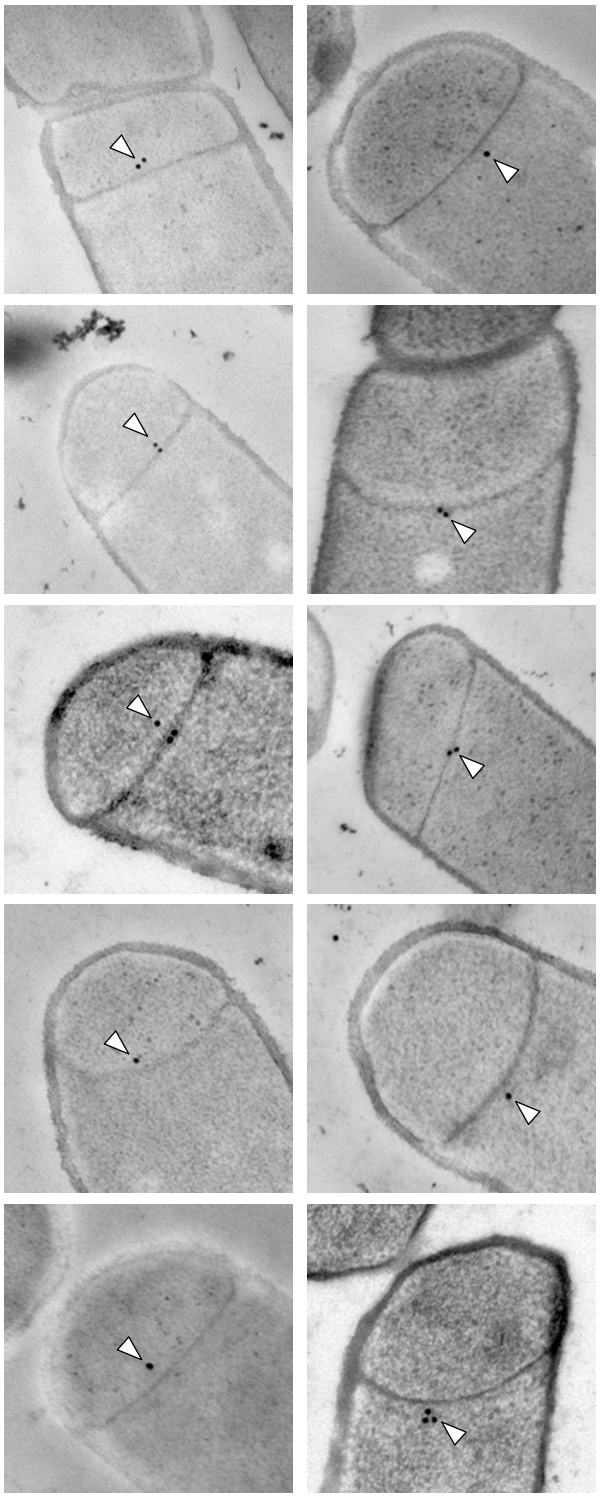

Supplemental Figure 9B (Burton et al.)

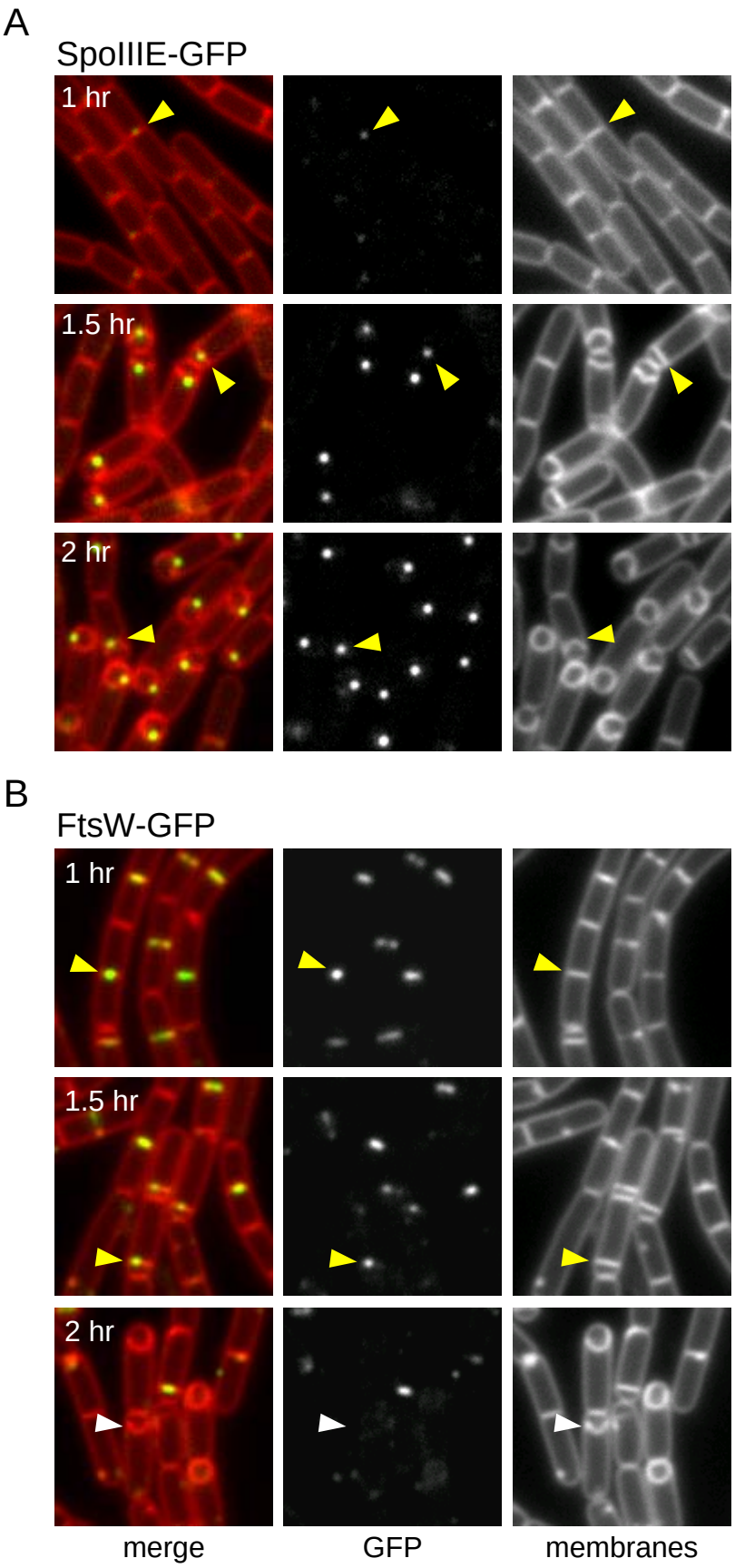

Supplemental Figure 10A&B (Burton et al.)

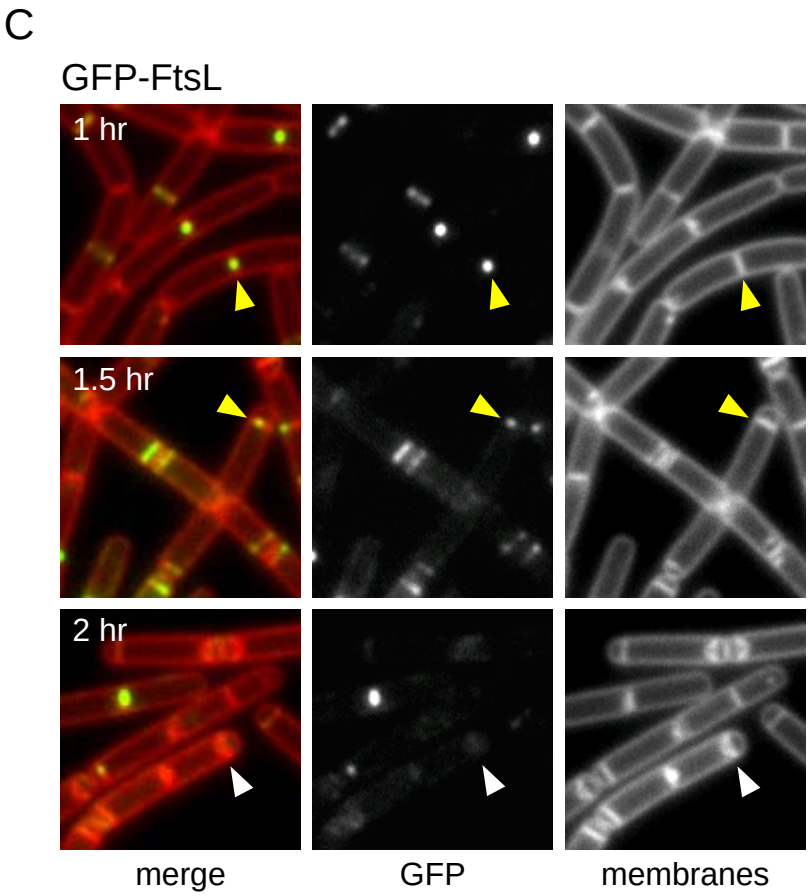

Figure S10. Division proteins are not retained at the sporulation septum during DNA translocation. Subcellular localization of (A) SpoIIIE-GFP (strain BDR1626), (B) FtsW-GFP (BKM1281), and (C) GFP-FtsL (strain BDR2200) at early times after the initiation of sporulation. In cells undergoing medial (1 hr) or polar (1.5 hr) division, FtsW-GFP and GFP-FtsL localize as discrete foci at the septal midpoint prior to the completion of cytokinesis (yellow caret). During DNA translocation (2 hr), both cell division proteins no longer localize to the polar septum (white caret). The absence of these division proteins during chromosome translocation suggests that cytokinesis is complete and that the division machinery is not involved in forming the translocation channel. For comparison, SpoIIIE-GFP foci are present at the site of DNA translocation (yellow caret). Occasionally, a weak SpoIIIE-GFP focus can be seen at the medial division plane (1 hr). This is presumed to be due to incomplete chromosome segregation prior to cytokinesis.

Table S1. Strains used in this study.

Strain	Genotype	Source/Reference
PY79	prototrophic strain	Youngman et al., 1983
BDR1050	spoIIIE36	Wu and Errington, 1994
BDR1626	spoIIIE-gfp (spec)	This work
BDR2200	trpC2, amyE::P_{xylA}-gfp-ftsL (spec), ftsL::neo	Sievers and Errington, 2000
BBB128	spoIIIE::spec, ycgO::spoIIIE (cat), yycR::P_{spoIIQ}-yfp (phleo), pelB::P_{spoIIQ}-cfp (kan)	This work
BBB131	spoIIIE::spec, ycgO::spoIIIE(D584A) (cat), yycR::P_{spoIIQ}-yfp (phleo), pelB::P_{spoIIQ}-cfp (kan)	This work
BBB162	ytzHΩpBB153[P_{spoIIQ}-cfp (spec)], yhdYΩpBB156[P_{spoIIQ}-yfp (cat)]	This work
BBB197	spoIIIE::spec, ycgO::spoIIIE(D584A)-gfp (cat)	This work
BBB213	spoIIIE::spec, ycgO::spoIIIE(D584A) (cat), yhdYΩpBB171[P_{spoIIQ}-cfp (kan)], ytzHΩpBB198[P_{spoIIQ}-yfp (phleo)]	This work
BBB339	spoIIQ::cat, spoIIIE:spec	This work
BKM776	spoIIIE::neo, ycgO::spoIIIE(cat)	This work
BKM778	spoIIIE::neo, ycgO::spoIIIE(D584A)(cat)	This work
BKM780	spoIIIE::neo, ycgO::spoIIIE(cat), spoIIR::tet	This work*
BKM784	spoIIIE::neo, ycgO::spoIIIE(cat), spoIIR::tet, zcc-82::spoIIR(94˚)(spec)	This work*
BKM786	spoIIIE::neo, ycgO::spoIIIE(cat), spoIIR::tet, zdd-85::spoIIR(123˚) (spec)	This work*
BKM788	spoIIIE::neo, ycgO::spoIIIE(cat), spoIIR::tet, zhb-83::spoIIR(-107˚) (spec)	This work*
BKM792	spoIIIE::neo, ycgO::spoIIIE(cat), spoIIR::tet, amyE::spoIIR(28˚) (spec)	This work*
BKM794	spoIIIE::neo, ycgO::spoIIIE(D584A)(cat), spoIIR::tet, zcc-82::spoIIR(94˚) (spec)	This work*
BKM796	spoIIIE::neo, ycgO::spoIIIE(D584A)(cat), spoIIR::tet, zdd-85::spoIIR(123˚) (spec)	This work*
BKM798	spoIIIE::neo, ycgO::spoIIIE(D584A)(cat), spoIIR::tet, zhb-83::spoIIR(-107˚) (spec)	This work*
BKM802	spoIIIE::neo, ycgO::spoIIIE(D584A)(cat), spoIIR::tet, amyE::spoIIR(28˚) (spec)	This work*
BKM820	spoIIIE::neo, ycgO::spoIIIE(cat), spoIIR::tet, zfg-83::spoIIR(213˚) (spec)	This work*
BKM822	spoIIIE::neo, ycgO::spoIIIE(cat), spoIIR::tet, zej-82::spoIIR (172˚) (spec)	This work*
BKM824	spoIIIE::neo, ycgO::spoIIIE(D584A)(cat), spoIIR::tet, zfg-83::spoIIR(213˚) (spec)	This work*
BKM826	spoIIIE::neo, ycgO::spoIIIE(D584A)(cat), spoIIR::tet, zej-82::spoIIR (172˚) (spec)	This work*
BKM986	yycR::$(tetO)_{120}$(cat), amyE::P_{spoIIE}-tetR-gfp(spec)	This work
BKM1247	amyE::P_{spoIIE}-tetR-gfp(spec), 130˚Ω$(tetO)_{240}$(cat)	This work
BKM1281	ftsW-gfp (spec)	This work
BKM1279	yycR::$(tetO)_{24}$(cat), amyE::P_{spoIIE}-tetR-gfp(spec)	This work
BKM1309	yycR::$(tetO)_{12}$(cat), amyE::P_{spoIIE}-tetR-gfp(spec)	This work
BKM1315	yycR::$(tetO)_{36}$(cat), amyE::P_{spoIIE}-tetR-gfp(spec)	This work
BNS276	spoIIIE36, yycR::P_{spoIIQ}-yfp (phleo), pelB::P_{spoIIQ}-cfp (kan)	This work
BTD1559	spoIIQ::cat	This work

* All ectopic *spoIIR* sites described (Zupancic et al., 2001).

Table S2. Plasmids used in this study.

Plasmid	Description	Source
pBB078	*ycgO::spoIIIE (cat)*	This work
pBB152	*P_{spoIIQ}-cfpΩyhdY (spec)*	This work
pBB153	*P_{spoIIQ}-cfpΩytzH (spec)*	This work
pBB155	*P_{spoIIQ}-yfpΩytzH (spec)*	This work
pBB156	*P_{spoIIQ}-yfpΩyhdY (cat)*	This work
pBB171	*P_{spoIIQ}-cfpΩydhY (kan)*	This work
pBB183	*ycgO::spoIIIE(D584A) (cat)*	This work
pBB198	*P_{spoIIQ}-yfpΩytzH (phleo)*	This work
pKM188	*yycR::$(tetO)_{120}$ (cat)*	This work
pKM212	*amyE::P_{spoIIE}-tetR-gfp (spec)*	This work
pKM245	*ftsW-gfp (spec)*	This work
pKM247	*yycR::$(tetO)_{12}$ (cat)*	This work
pKM248	*yycR::$(tetO)_{36}$ (cat)*	This work
pNS051	*yycR::P_{spoIIQ}-yfp (phleo)*	This work
pNS056	*pelB::P_{spoIIQ}-cfp (kan)*	This work
pTD126	*spoIIQ::cat*	This work

Table S3. Oligonucleotides used in this study.

Oligonucleotides used for PCR

Primer	**Sequence***
oBB162	gtcagaattcgtcggacaggcaatcaat
oBB163	gactggatccggcagcttttccttctcagt
oBB181	caggatccgacccgcaagctcgtttttc
oBB182	gtctgcagaatggcttggtatgtgttatctga
oBB183	caggatccgcgctcttgtgttggggtctttg
oBB184	gtctgcaggttctcaatcggcgtagcgtagg
oDR78	gccggatccttatttgtatagttcatccatgcc
oDR107	ggcaagcttacataaggaggaactactatgagtaaaggagaagaac
oDR188	gccaagcttacataaggaggaactactatgtctagattagataaaagtaaagtg
oDR459	cggctcgagcattacagtttacgaaccgaacagg
oDR573	gcgaagcttagactctagcaaggcatgacatc
oDR574	gcgaagcttgcagcctctagcagtatggacg
oDR575	gccgaattctgtcattgctgaagagctcggc
oDR577	cggctcgagcagataaacagttttttgagctg

**restriction endonuclease sites are underlined.*

Oligonucleotides used for site-directed mutagenesis

Name	Sequence*	Mutation
oBB148	cattgtggacgagctagccg**c**tctcatgatggtcgcttcatc	spoIIIE^{D584A}
oBB149	gatgaagcgaccatcatgaga**g**cggctagctcgtccacaatg	spoIIIE^{D584A}

**mutated nucleotides in bold face.*